Modeling of Casting, Welding and Advanced Solidification Processes - XI
Edited by Charles-André Gandin and Michel Bellet
TMS (The Minerals, Metals & Materials Society), 2006

INTEGRATED DESIGN OF STEEL CASTINGS FOR SERVICE PERFORMANCE

Richard. A. Hardin[1], Richard K. Huff[2] and Christoph Beckermann[1]

[1]Dept. of Mech. and Ind. Eng., 3131 S.C., The University of Iowa, Iowa City, IA 52242, USA
[2]Caterpillar Inc., Champaign, IL 61820, USA

Keywords: steel casting, porosity, fatigue life, modeling, radiography

Abstract

An integrated approach is presented for the design of structural components made of steel castings that couples casting simulation with stress and fatigue simulation of the part in service. The casting simulation is used to predict the location, size, and shape of porosity defects in the part. The porosity predictions are then transferred to finite element stress analysis and fatigue analysis codes in order to predict the strength and fatigue life of the part in the presence of porosity. Strength and fatigue measurements on test specimens cast with varying levels of porosity are performed to establish relations between the mechanical properties and the porosity; in particular, it is shown how the elastic modulus and the fatigue notch factor depend on the size and shape of the porosity. An industrial case study is used to validate the present simulation methodology. The case study illustrates that a large pore in a low stressed area of the casting may be far less detrimental than a small amount of microporosity in an area that is subject to high tensile stresses. The proposed integrated approach leads to the design of more reliable castings, tailored inspection standards, and decreased reliance on factors of safety.

Introduction

Effects of shrinkage discontinuities on the structural performance of carbon and low alloy steel castings are not well understood. There are currently no standard or well-accepted methods of analysis that engineers use to determine the effect of porosity on mechanical performance of steel castings. Similarly, there are no guidelines relating non-destructive testing or non-destructive examination (NDT or NDE) methods, such as radiography, to the performance of cast steel components. Unless design engineers have ample test data and/or a track record of experience for a given part, they request that castings pass specified NDT standards without knowing exactly how this translates to part performance. As a result, integration of casting soundness information into the design of castings is still ad-hoc, based on case-by-case experience. Progress on the topic has not advanced much beyond this point despite great interest for many years [1-8]. Usually, the benefits of design experience and performance data are available only for long-run, mass-produced components. Having such a knowledge-base for all steel castings through computer modeling, will lead to more confidence in casting designs, a more rational use of testing specifications, and better performing castings. Developing such engineering guidelines in a design approach that integrates knowledge about the effects of porosity into casting design, production and NDT is the goal of the present work.

The integrated casting simulation/performance analysis and design process envisioned is shown schematically in Figure 1. This process enables simultaneous optimization of the casting process parameters (e.g., riser location) and the component geometry (e.g., section thickness) at an early stage in the product definition. Durability prediction in the presence of porosity is possible if

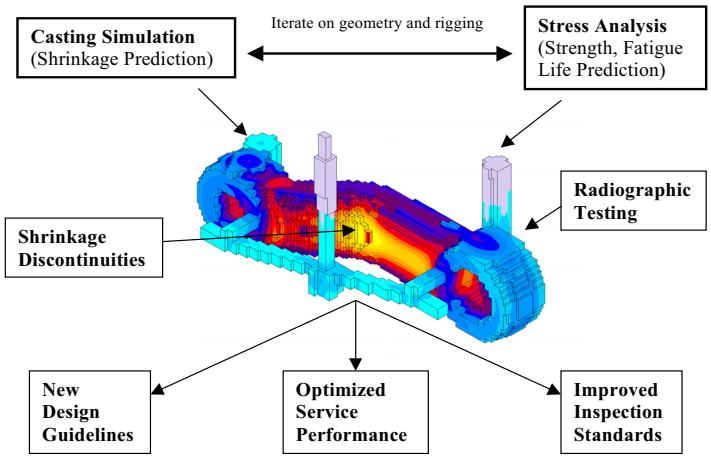

Figure 1. Illustration of integrated design of steel castings for service performance concept.

casting simulation codes can predict not only the amount, location, and distribution, but also the size and shape of porosity. The smooth surface of a gas pore will very likely behave differently than the jagged surface of dendrites associated with a macro-shrinkage produced cavity. More recent literature demonstrates the methods being proposed to address the "Stress Analysis" component of Figure 1 [9-16]. The "Casting Simulation" component is lagging somewhat. Even accurately predicted average volumetric porosity is insufficient for use in performance prediction; it does not give the information on pore size and shape necessary to apply fatigue models. Recent developments in casting process simulation [17] allow for prediction of porosity due to gas-related and shrinkage-driven mechanisms, and physically realistic pore nucleation and growth modeling result in prediction of characteristic pore size and shape, in addition to more accurate volumetric porosity prediction. Such information, now available from casting simulation, can be integrated into casting mechanical performance modeling. Provided the necessary strength/fatigue models and property data exist for incorporation of the casting simulation results, computational tools can be developed to design high performance steel castings with increased confidence.

A thorough review of literature in the area of component life prediction in the presence of porosity is given in [18-19]. The most commonly used methods to predict the fatigue life of castings with porosity are [20]: 1) Modeling pores as "equivalent" notches or cracks and determining the local strain arising from the effect of the notch and applying strain-life (or ε-N) concepts to predict fatigue life. 2) Modeling the porosity as pre-existing cracks within the component, and using linear elastic fracture mechanics (LEFM) to predict crack propagation [20, pp.122-173].

Method 1) is termed "crack initiation" life prediction. When used alone, one assumes that crack initiation consumes the majority of the fatigue life. Component life predictions using Method 2) alone assume crack propagation consumes most of the life. Combining both methods of prediction produces the so-called "total life" of the component, "initiation life" plus "propagation life".

Method 1) is the older of the two methods [3-4]. Typically these strain-life models are thought to predict the duration of life to initiate a crack on the order of 1 mm. By this concept, one determines the crack initiation life in the presence of porosity by modeling the pore as a notch. Researchers studying aluminum castings have treated pores in castings as notches to predict the effect of porosity on crack initiation life and the mechanism of crack formation from pores [10,14]. The second stage of fatigue life, the "fatigue crack growth" stage represented by

Method 2) and LEFM, has a critical role in damage-tolerant design life prediction. The crack pre-exists, formed either from fatigue or during manufacturing of the part. It has found application analyzing the life of cast components with porosity. LEFM with application to steel castings is given in [8], and recently fatigue life investigations for a variety of cast metals by fracture mechanics approaches are available: for nodular cast iron [13,15], cast aluminum alloys [12,14], and steel alloys [7,9,11,16,21]. Modeling and experimental studies on the effect of steel casting defects and porosity on fatigue life using fracture mechanics and crack growth models are reviewed in [11]. Reductions in fatigue strength of 35% and 50% are observed for "sizes" (areas of cavities) of less than and greater than 3 mm^2, respectively [7]. For low alloy steel, fatigue strength reductions from 8 to 30% were found when shrinkage porosity cavities covered 3 to 7% of the fracture surface [21]. A comparison between the measured fatigue life of test specimens containing casting defects (porosity and inclusions) and the fatigue life obtained by modeling the specimen using crack initiation (local strain and stain life concepts) and crack propagation (fracture mechanics) approaches has been presented [9]. In the crack initiation model the defects were considered to be 3-D notches, and in the crack growth model the defects were treated as 2-D elliptical cracks having an envelope about the defect. It was found [9] that the crack initiation estimate of life was more accurate than the fracture mechanics approach, and that interpreting the porosity as pre-existing cracks resulted in too conservative an estimate of the fatigue life. Dabayeh and Topper [12] came to a somewhat different conclusion for cast aluminum where the local strain approach gave quite un-conservative estimates of fatigue life, and the crack growth method gave better agreement.

Quantitative measurement of the porosity in 8630 steel test specimens based on radiographs taken of the specimens before testing is presented. The radiography of the specimens, their measured fatigue life, and fatigue notch factors determined from strain-life calculations of the specimens are analyzed. Finally, an example analysis for a casting application is presented.

Experimental and Analytical Procedures

Details of the production and testing of the AISI 8630 quenched and tempered cast steel specimens are given elsewhere [18]. Three levels of macroporosity severity, large enough to be detected by radiographic inspection, were designed into the castings using casting simulation as shown in Figures 2 a) and b). In an earlier study [22], specimens were machined from large cast trapezoidal-shaped keel blocks, and we refer to this as "sound" test data. Fatigue testing to determine the cyclic and fatigue properties of the specimens with porosity was performed according to ASTM E 606 [23]. Digital radiography (8-bit gray level, 1200 dots per inch) of the

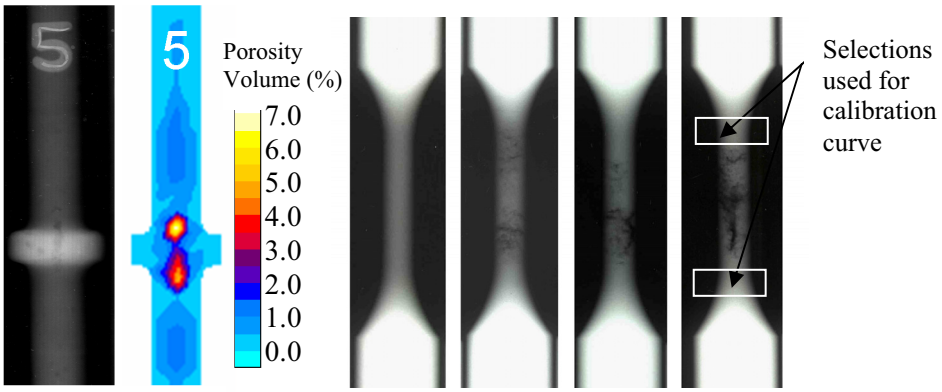

Figure 2. Comparison between (a) radiograph of specimen casting and (b) computer model predictions of specimen porosity volume percentage, and specimen radiographs of machined fatigue test specimens with c) microporosity, d), e), and f) are specimens with "least", "middle", and "most" macroporosity, respectively.

fatigue test specimens was performed at Alloy Weld Inspection Co., Bensenville, Illinois using a Fuji digital x-ray system. Example results of the radiographs for the range of porosities analyzed in this study are shown in Figures 2 c) to f) for specimens with microporosity, and "least", "middle", and "most" macroporosity specimens. Two orthogonal radiographic views of each specimen group were shot. A method to quantitatively measure the porosity in the specimens and determine the porosity distribution in the specimen matching the measurements in the two x-ray views was devised [19]. The porosity at any cross-section along the specimen length can be determined from the "lost thickness" t_{lost} measured on the x-ray as shown in Figure 3 for the two orthogonal radiographic views of a specimen. The distributions of lost cross-sectional area along the specimen length show excellent agreement, demonstrating good reproducibility. The position of the smallest sectional area is indicated; it agrees well with the apparent lost cross-sectional area derived from the measured specimen modulus. The reconstructed porosity from the two x-ray views is shown in Figure 4 a), and shows good agreement with observations from cut sections considering it is determined from only two views.

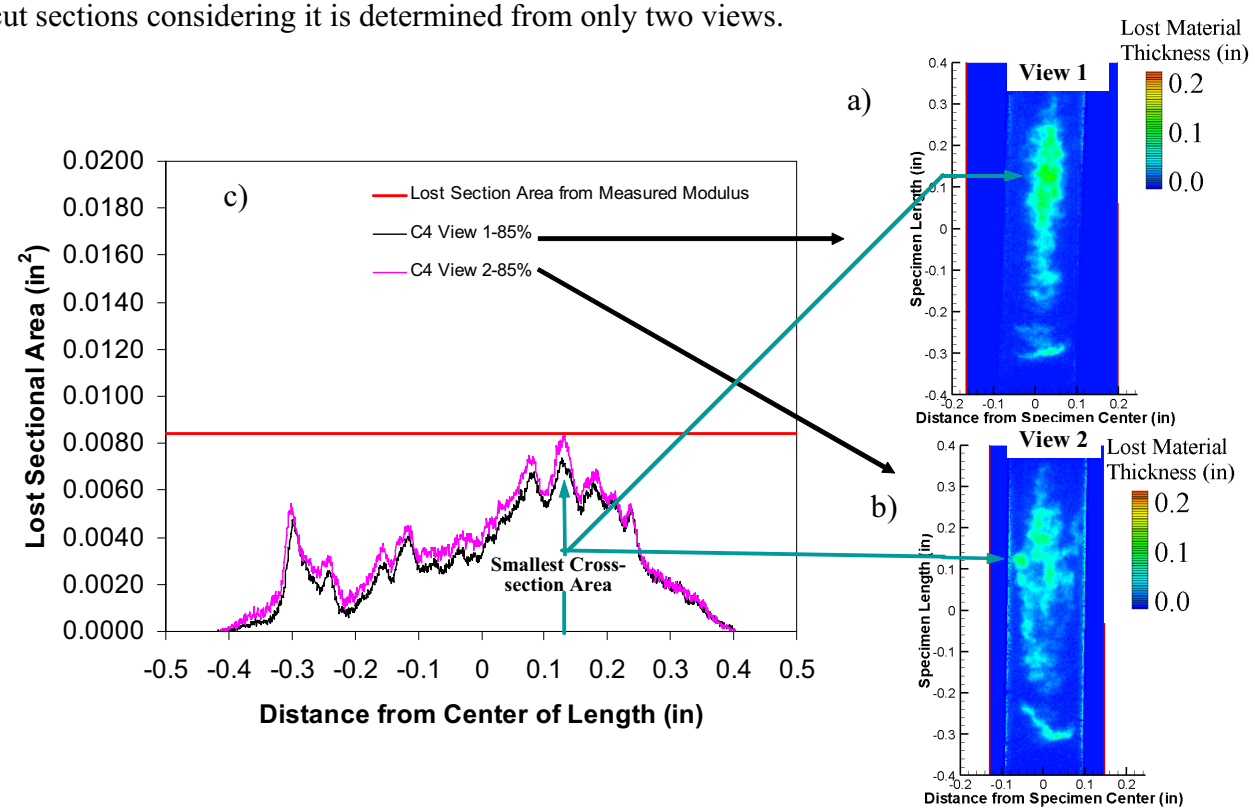

Figure 3. Distributions of lost material thickness for a specimen as measured from two orthogonal views a) and b), and c) the lost sectional area versus position along the specimen length for the two views. Lost section area determined from the measured specimen modulus E_{meas} is indicated.

Results: Comparison between Fatigue Tests and Radiographic Analysis

The measured modulus of elasticity E_{meas} was determined from the stable cycle hysteresis loops during fatigue testing. This correlated well with the maximum section porosity from the radiographic analysis as shown in Figure 4 b). Space limitations here require that the reader find the details of the fatigue testing, and comparisons with methods of fatigue life calculations, elsewhere [18,19]. In Figure 5 a) and b) micropores having 10 to 200 μm size on the surface of microporosity specimens are shown. Strain-life calculations on sound material having spherical notches of 10 to 200 μm diameter produced the curves shown in Figure 5 c) showing good agreement with the data. Stress-life data for tests on specimens with macroporosity are compared with the microporosity data curve-fit in figure 6 a). Specimens containing macroporosity had

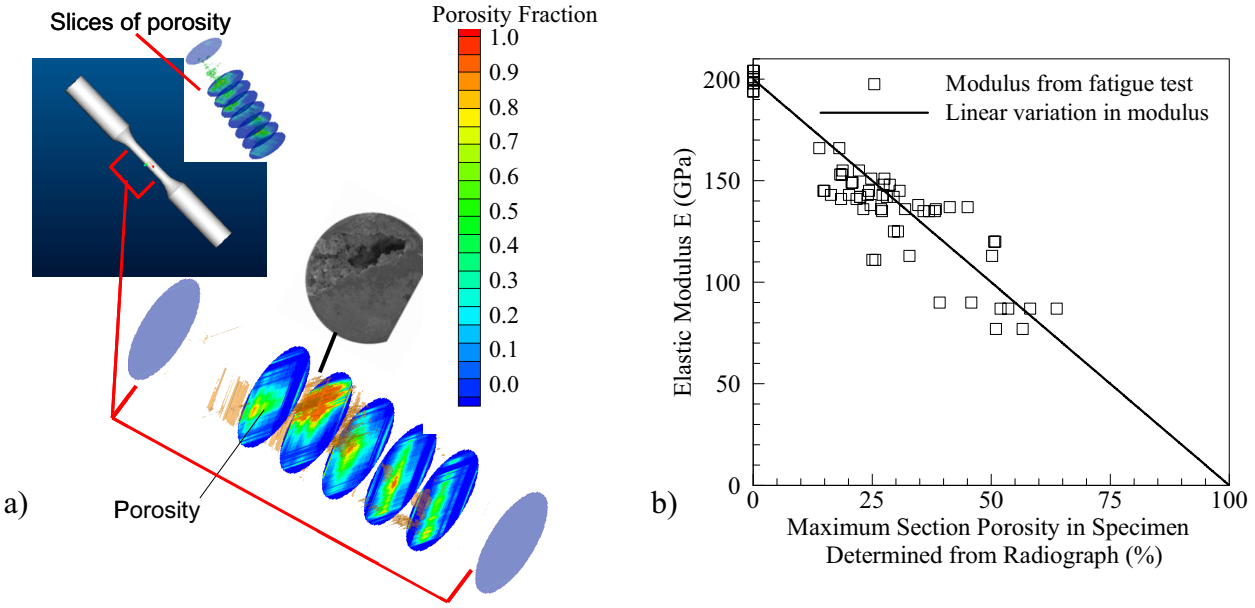

Figure 4. a) Slices of reconstructed porosity distribution from radiographs and corresponding section from a cut specimen, b) measured elastic modulus from fatigue testing compared with the maximum sectional porosity measured from radiographs.

much lower fatigue lives. The stress amplitude has been increased to account for the reduced elastic modulus of the macroporosity specimens. Scatter observed in the macroporosity specimens is due primarily to the fatigue notch factor K_f effect which varies from specimen to specimen depending on the characteristic porosity size and shape.

Handbook stress concentration factors (K_t gross area) and the fatigue notch factors determined from the fatigue test results and conditions (by back-calculation of the strain-life equations) were compared [19]. In general $K_f \leq K_t$, where equality denotes that the material is fully notch sensitive. The stress concentration factor for a cylinder with a spherical hole depends upon the hole-to-bar diameter ratio (d/D) [24]. The maximum lost section thickness in the cross-section of maximum porosity was the characteristic dimension used as d in the comparison between the

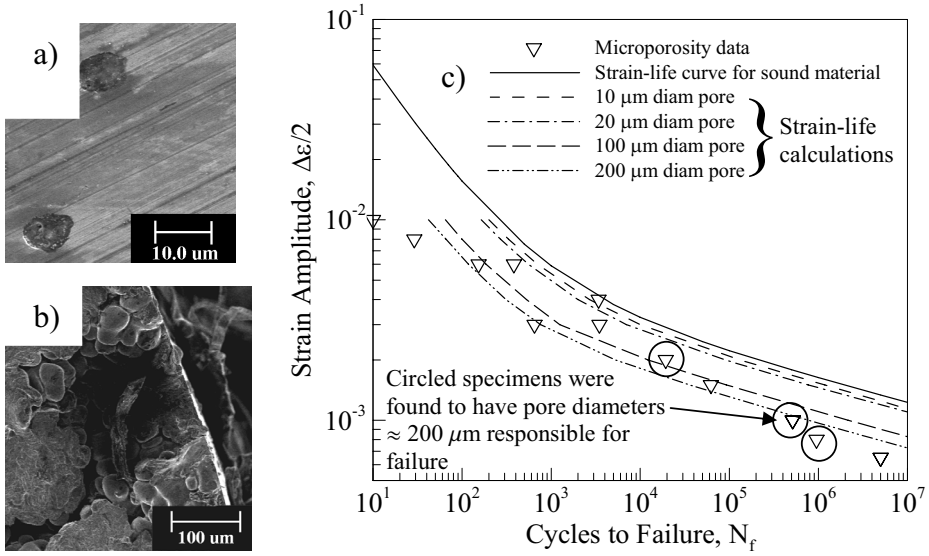

Figure 5. Typical micropores found in specimens with microporosity a) on polished cut surfaces and b) on fracture surfaces, and c) strain-life test data and calculations for micropores modeled as notches.

handbook K_t and the measurements. Plotted as the ratio of porosity dimension to specimen diameter ratio, a good correspondence in trend and magnitude with the handbook stress concentration factor relationship for the spherical hole in cylinder was found, as shown in Figure 6 b). The K_f back calculated from the measurements appears to make good physical sense compared to a handbook stress concentration factors.

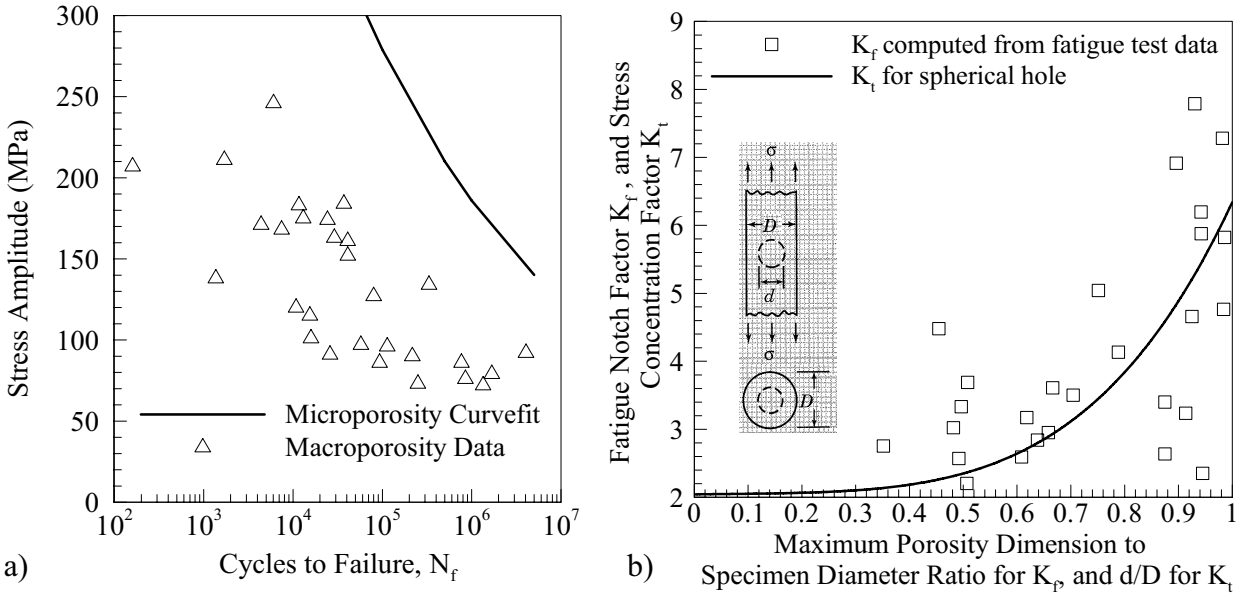

Figure 6. a) Stress-life curve for specimens with macroporosity compared with microporosity data curve, b) Fatigue notch factor K_f calculated from fatigue test data versus maximum porosity dimension measured from radiographs compared with stress concentration factor K_t for spherical hole in round bar.

Using new casting process models that predict porosity amount and size [17], this approach to casting service performance simulation is now being tested on production castings. As shown in Figure 7 a), casting simulations are performed first to predict the porosity field. Based on the porosity amount and size, the fatigue notch factor distribution in the part is determined. Handbook [24] and fatigue-test derived relationships for the fatigue notch factor versus porosity characteristics (amount and size) are being tested and developed. Finite element stress calculations are performed on the part using porosity-dependent elastic modulus to reflect the bulk loss in material strength observed in the testing presented here. The finite element modeling is performed at design loads to develop dynamic history for strain-life fatigue modeling. A cycle of in-service loading is defined and the strain-history of a cycle is computed. The strain-history for a cycle is then input to strain-life calculations including the fatigue notch factor [18,19] and the fatigue life with porosity is calculated (Figure 7 c). For comparison purposes, the fatigue life without porosity is shown in Figure 7 d). This case study illustrates that large regions of porosity in low stressed areas of the casting may be far less detrimental than a small amount of microporosity in an area that is subject to high tensile stresses, the "location of greatest concern" shown in Figure 7.

Summary and Conclusions

A method for measuring porosity from radiographs of fatigue test specimens was developed. Measured porosity dimensions from the radiographs were found to agree well with observations made on specimen surfaces. The specimen porosity measurement can be summed up over the specimen cross section to determine the cross-sectional porosity versus length distribution along the specimens. Cross-sectional porosity distributions determined from two radiographic views of the specimens show excellent agreement, and demonstrate the method's

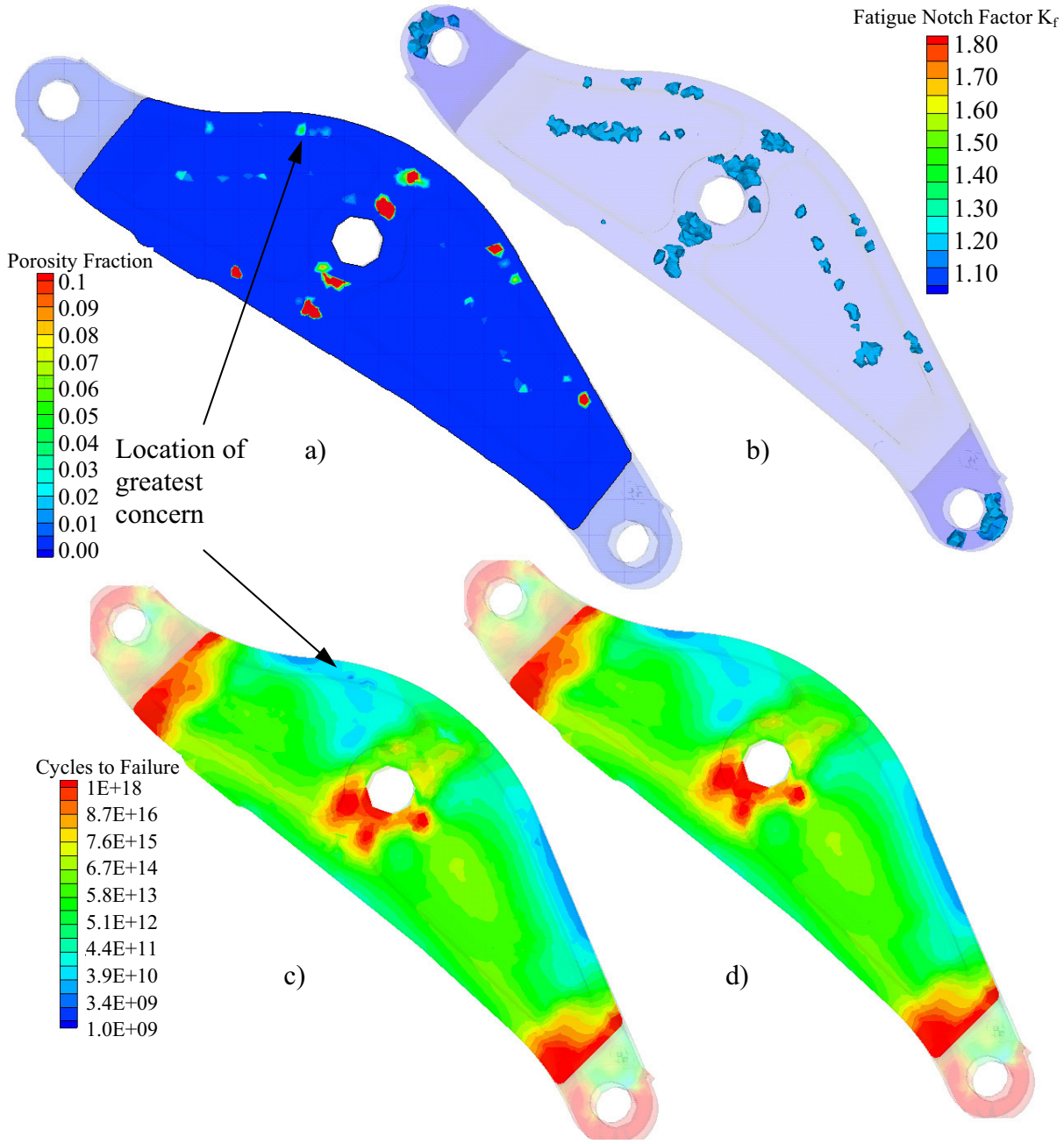

Figure 7. Example of test case application of service performance prediction for a casting with porosity; a) prediction of porosity at a cross-section in the part from MAGMAsoft, b) x-ray view of fatigue notch factor distribution in casting determined from porosity field, c) fatigue life prediction using notch factors from porosity field, fatigue life prediction using no porosity data (i.e. $K_f = 1$ throughout part).

repeatability. The maximum cross-sectional porosity in the radiographs was found to correlate well with the fatigue test specimens' measured elastic modulus. Converting the elastic modulus measurements to an apparent porosity in the specimen, a close one-to-one correspondence was found between this and the maximum cross-sectional porosity in the specimens. The maximum cross-sectional porosity found in the specimens in this study ranged from about 15% to 65% based on the radiographic analysis. Fatigue test results were compared with the radiographic analysis by determining the fatigue notch factors of the test specimens based on their measured fatigue lives, test conditions, measured elastic modulus and other properties. Comparisons between the notch factor and porosity from the radiographs showed a good correlation, but this

result is specific to the test geometry used. Using a maximum radiographically measured porosity dimension to specimen diameter ratio, comparison with textbook stress concentration factors showed the fatigue test result correlate with the K_t relationship for a spherical hole in a round bar. The effect of the porosity size on fatigue and fatigue test results appear to be meaningful in the context of handbook values. The authors present and example application of service performance prediction for a casting to demonstrate the importance of considering both porosity and service conditions in part design. Regions with large amounts of porosity are found to not affect fatigue life as much as more highly stressed regions with microporosity.

Acknowledgements

This work was sponsored by the Defense Supply Center Philadelphia, Philadelphia, PA, Defense Logistics Agency, Ft. Belvoir, VA, the Army Research Laboratory, and Caterpillar Inc..

References

1. H.R. Larson et al., *AFS Transactions*, 100 (1959), 676-684.
2. J.F. Wallace et al., (Steel Foundry Research Foundation Report, SFRF, 1962).
3. H. Greenberg, *Trans. of the ASME Journal of Basic Engineering*, 87 (4) (1965), 887-893.
4. R. E. Peterson, *Trans. of the ASME Journal of Basic Engineering*, 87 (4) (1965), 879-886.
5. C. Vishnevshy, M. Bertolino, and J.F. Wallace, (Steel Foundry Research Foundation Report, SFRF, 1967).
6. J.F. Wallace et al., (Steel Foundry Research Foundation Report, SFRF, 1969).
7. M. Kohno and M. Makioka, *AFS Transactions*, 78 (1970), 9-16.
8. W.J. Jackson, (Steel Founders' Society of America, 1978).
9. P. Heuler, C. Berger, and J. Motz, *Fatigue Fracture Engng. Mater. Struct.*, 16 (1) (1992), 115-136.
10. C. Sonsino and J. Ziese, *Int. Journal of Fatigue*, 15 (2) (1993), 75-84.
11. S. Jayet-Gendrot, P. Gilles, and C. Migne, *Fatigue and Fracture: 1997 PVP-Vol. 350*, ASME, 1 (1997) 107-116.
12. A. Dabayeh and T.H. Topper, *Fatigue Fracture Engng. Mater. Struct.*, 23 (2000), 993-1006.
13. T. Mansson and F. Nilsson, *Int. Journal of Cast Metals Research*, 13 (2001), 373-378.
14. J-Y. Buffiere et al., *Materials Science and Engineering A,* 316 (2001), 115-126.
15. Y. Nadot and V. Denier, *Engineering Failure Analysis*, 11 (2004), 485-499.
16. T. Billaideau, Y. Nadot and G. Bezine, *Acta Materialia*, 52 (2004), 3911-3920.
17. K.D. Carlson et al., *Proceedings of Modeling of Casting, Welding and Advanced Solidification Processes X*, (May 25-30, Destin, Florida, 2003), 295-302.
18. K.M. Sigl et al., "Fatigue of 8630 Cast Steel in the Presence of Shrinkage Porosity," *International Journal of Cast Metals Research*, 17 (3) (2004), 130-146.
19. R. Hardin and C. Beckermann, *Proceedings of the 58th Technical and Operating Conference* (SFSA, Chicago, Illinois, 2004).
20. R.I. Stephens et al., *Metal Fatigue in Engineering*, John Wiley and Sons, 2001.
21. K. Chijiwa, T. Nakayama T. and Imamura M., *CIF*, 36, 1-12.
22. R. I. Stephens, *Fatigue and Fracture Toughness of Five Carbon or Low Alloy Cast Steels at Room or Low Climatic Temperatures* (Carbon and Low Alloy Technical Research Committee, Steel Founders' Society of America, Des Plaines, IL, 1982).
23. Standard E606, *2002 Annual Book of ASTM Standards* (American Society of Testing and Materials, West Conshohocken, PA 2002), 30 (1), 569-583.
24. R. E. Peterson, *Stress Concentration Factors*, Wiley-Interscience, New York, 1974, 221.